Hyperfine Interactions (2004) 159:55–61
DOI 10.1007/s10751-005-9081-8
© Springer 2005

Structural Properties of the Donor Indium in Nanocrystalline ZnO

T. AGNE[1,*], M. DEICHER[1], V. KOTESKI[2], H.-E. MAHNKE[2], H. WOLF[1] and T. WICHERT[1]
[1]*Technische Physik, Universität des Saarlandes, 66041, Saarbrücken, Germany*
[2]*Bereich Strukturforschung, Hahn-Meitner-Institut Berlin, 14109, Berlin, Germany;*
e-mail: Thomas.Agne@tech-phys.uni-sb.de

Abstract. The structural properties of the nanocrystalline semiconductor ZnO (nano-ZnO) doped with the donor Indium were investigated by perturbed γγ angular correlation spectroscopy (PAC) and extended X-ray absorption fine structure measurements (EXAFS). Up to an average concentration of one In atom per nanocrystallite, PAC measurements show that about 12% of the ^{111}In atoms are incorporated on substitutional Zn sites. At higher In concentrations, new In defect complexes are visible in the PAC spectra, which dominate the spectra if the average In concentration exceeds one In atoms per nanocrystallite. In addition, the local environment of Zn and In atoms in In doped nano-ZnO was investigated by EXAFS. The measurements at the K edge of Zn show that the crystal structure of nano-ZnO corresponds to bulk ZnO. In heavily In doped nano-ZnO the EXAFS experiments at the K edge of In exhibit an expansion of the first O shell about the In site. Since about four O atoms are detected in this first shell a substitutional incorporation of the In atoms in the ZnO lattice is suggested. The second shell to be occupied by Zn atoms as well as higher shells are almost invisible, which might have the same microscopic origin as the occurrence of defect complexes observed by PAC.

1. Introduction

In nanometer scale semiconductors, several optical and electrical properties exhibit a strong size dependence [1]. The doping of nanocrystalline semiconductors, which is the basis for the successful application of semiconductors, still poses a severe problem [2]. Most effort for solving this problem has been focused on II–VI semiconductor nanocrystals that were doped with impurities, such as Mn, Cu, or rare earth-elements, such as Tb (Ref. 2 and references therein). The doping with impurities that introduce shallow donor or acceptor levels has been reported by only a few groups [3–5].

In a previous work, we reported on nanocrystalline ZnO (nano-ZnO) with a mean grain size of 11 nm, which was successfully doped with the radioactive donor ^{111}In [5]. The required incorporation of ^{111}In atoms on undisturbed Zn sites after a hydrothermal treatment at 473 K was shown by detecting the site

* Author for correspondence.

specific electric field gradient (EFG) in nanocrystalline ZnO using perturbed γγ angular correlation spectroscopy (PAC) [6]. At 473 K, the crystalline quality of nano-ZnO is significantly improved as revealed by different experimental techniques (TEM, XRD, UV–VIS absorption, and photoluminescence spectroscopy). The analytical results indicate that the successful doping of nano-ZnO with In donors at 473 K is accompanied by the onset of crystal growth and might be accompanied by the removal of intrinsic defects in the nanocrystallites. Based on the known experimental conditions for the incorporation of ^{111}In atoms in nano-ZnO, experiments with stable In atoms as a function of In concentrations are possible, now.

In this work, the structural properties of nano-ZnO doped with the donor Indium in a range of the relative In concentration [In/ZnO] of $10^{-5} - 10^{-3}$ are presented. The environment of the In atoms in In doped nano-ZnO is investigated by PAC using the probe ^{111}In/^{111}Cd. Additional information on the local structure of In and Zn atoms in In doped nano-ZnO is obtained by extended X-ray absorption fine structure measurements (EXAFS). For the latter experiment a relative In concentration of at least 10^{-3} is required.

2. Sample preparation

In doped nano-ZnO samples were produced by electrochemical deposition under oxidizing conditions (EDOC) [7, 8]. The electrolysis process uses dissolved Zn^{2+} ions and takes place in a solution of 0.1 M tetrabutylammonium-bromide (TBA-Br) dissolved in 2-propanol. During the electrolysis a current density of 10 mA/cm^2 was applied at a temperature of about 303 K. The nano-ZnO crystallites were doped *in situ* with In atoms by adding a solution of stable In along with radioactive ^{111}In atoms to the electrolyte. During this procedure the ZnO clusters are coated with TBA, which works as a stabilizer of the colloidal nanocrystallites. In this way it was possible to obtain relative concentrations of In atoms in the range between 10^{-6} and 10^{-3}, which were verified by chemical analysis. For hydrothermal treatment, the ZnO nanocrystals were dissolved in 2-propanol and the solution, encapsulated into a pressure vessel was heated to a temperature of 473 K, yielding a pressure of about 2.5 MPa. After that treatment the ZnO nanocrystallites have a volume-weighted mean grain size of 11 nm.

3. PAC experiments

In ZnO, the incorporation of the ^{111}In atoms on Zn sites can easily be verified by comparing the electric field gradient (EFG), measured at the site of the radioactive dopant ^{111}In/^{111}Cd in a PAC experiment [6], with the well-known EFG caused by the hexagonal ZnO lattice at the probe ^{111}In/^{111}Cd on a Zn site. Choosing V_{zz} as the largest component of the traceless EFG tensor and the asymmetry parameter $\eta = (V_{xx} - V_{yy})/V_{zz}$, the EFG measured by the probe ^{111}In/^{111}Cd in bulk ZnO is characterized by the coupling constant $\nu_Q = eQV_{zz}/$

h = 31.2(1) MHz and η = 0 [9]; here, Q is the nuclear quadrupole moment of the isomeric 245 keV $-$ $5/2^+$ level of ^{111}Cd used for measuring the nuclear quadrupole interaction.

For In doped nano-ZnO with relative In concentrations of 10^{-5}, 10^{-4}, and 10^{-3}, Figure 1 shows PAC spectra (left) along with their Fourier transforms (right); the corresponding average numbers of In atoms per nanocrystallite n_{In} are (top to bottom) 0.1, 1, and 10, respectively. Up to a concentration of 10^{-4} (n_{In} = 1) an EFG characterized by ν_Q = 31(2) MHz and η = 0.2(1) is observed, which is detected by a fraction of about 12% of the ^{111}In atoms. The coupling constant ν_Q matches well to that of the EFG of ^{111}In on undisturbed Zn sites in bulk ZnO, mentioned above. The difference in the asymmetry parameter η of the observed EFG might indicate distortions of the ZnO lattice in the environment of the ^{111}In atoms. These distortions can be caused by the incorporation of ^{111}In atoms near the surface of the crystallite or by internal strain present in the nanocrystallites. The existence of lattice distortions in nanocrystallites has been confirmed by EXAFS experiments [10]. At the relative concentration of 10^{-4} obviously new perturbations arise in the PAC spectra, which are characterized by two EFGs with the parameters ν_Q = 130(10) MHz, η = 0.4(1) and ν_Q = 150(12) MHz, η = 0.7(1). These parameters are detected by 17% and 14% of the probe atoms, respectively. The new EFGs are assigned to In defect complexes. At still higher In concentration of 10^{-3} (n_{In} = 10), the PAC spectrum exclusively exhibits the EFGs of the In defect complex, whereas the signal of In atoms located on unperturbed Zn sites has totally vanished. The observation of the various EFGs in the PAC spectra of In doped nano-ZnO is obviously closely connected with the actual In concentrations in the ZnO nanocrystals. Finally, it should be noted that in all experiments the majority of In atoms (70–80%) is exposed to a wide distribution of EFG leading to a strong relaxation in the PAC spectra. These In atoms might by located in defect-rich surroundings, e.g. surface sites or dislocations.

The appearance of additional EFGs at In concentrations of 10^{18} cm^{-3} (corresponding to a relative In concentration of $\sim 10^{-4}$) and above was also observed in the II–VI compounds CdTe, ZnTe, ZnSe, CdSe, CdS, ZnS [11]. In the case of CdTe, these EFGs were caused by Cd vacancies [12].

4. EXAFS experiments

The local structure of In and Zn atoms in In doped nano-ZnO was investigated by EXAFS measurements at a temperature of 20 K in fluorescence mode at the X1 beam line of HASYLAB at DESY. The analysis of the absorption spectra was done following the standard FEFF procedure [13–16].

The EXAFS results are plotted in Figure 2: Panel (b) shows the K edge absorption $\chi(k)$ at the Zn host atoms together with its Fourier transform (FT). The data can be fitted up to the fourth nearest-neighbour shell with parameters known from bulk ZnO (see Figure 2(a)). The fit parameters of the first O shell

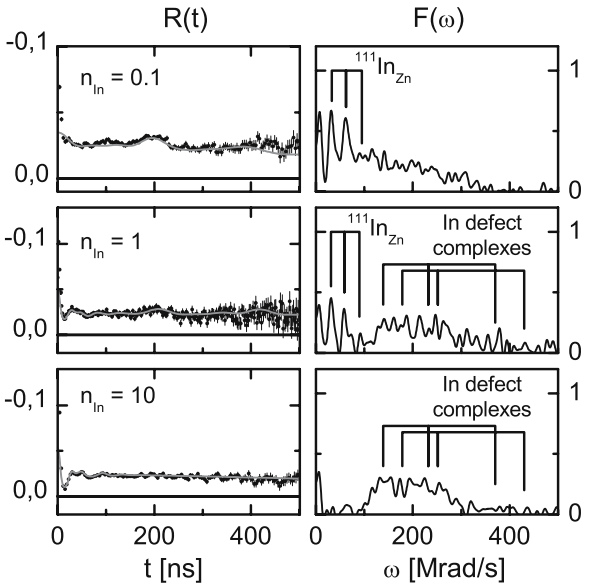

Figure 1. PAC spectra (left) and their Fourier transforms (right) of nanocrystalline ZnO doped with the donor In at different average number of In atoms per crystallite (n_{In}).

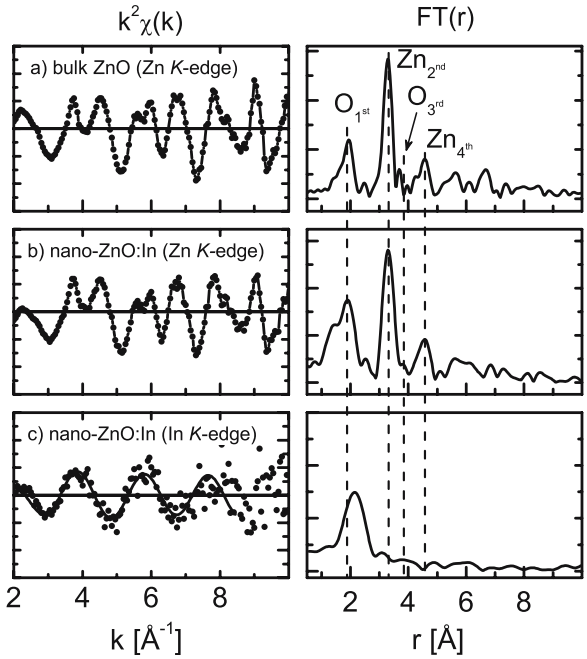

Figure 2. EXAFS spectra (left) and their Fourier transforms (right) of (a) bulk ZnO measured at 20 K at the K edge of Zn and of In doped nano-ZnO ([In/ZnO] = 10^{-3}) measured at the K edges of (b) Zn and (c) In.

Table I. Fit parameters of EXAFS experiments performed at the K edges of Zn and In in bulk ZnO and highly In doped nano-ZnO

Sample	Absorber	$O_{1st\ shell}$			$Zn_{2nd\ shell}$		
		n	R (Å)	σ^2 (10^{-3}Å^{-2})	*n*	R (Å)	σ^2 (10^{-3}Å^{-2})
Bulk ZnO	Zn	4.1 ± 0.2	1.96 ± 0.01	2.6 ± 0.2	11.9 ± 0.3	3.23 ± 0.01	2.6 ± 0.8
Nano-ZnO:In	Zn	3.5 ± 0.8	1.96 ± 0.02	3.0 ± 1.5	11.3 ± 1.0	3.22 ± 0.02	4.3 ± 0.6
Nano-ZnO:In	In	3.3 ± 1.4	2.17 ± 0.05	4.01 ± 7.9	–	–	–

n number of atoms; *R* distance to the absorber atom; σ^2 rms fluctuation in the distance.

(O_{1st}) and the second Zn shell (Zn_{2nd}) are listed in Table I together with the corresponding parameters of ZnO bulk material [17]. Figure 2(c) shows the K edge absorption $\chi(k)$ at the In dopant atoms along with its Fourier transform. In the FT spectrum the first O shell (O_{1st}) is clearly visible, whereas the atoms in the second Zn shell (Zn_{2nd}) and higher shells are almost invisible. An analysis of the first O shell about the In atoms yields the radial distance of about 2.17(5) Å (Zn–O_{NN}: 1.96(1) Å), which seems to be caused by the larger covalent radius of the In atoms as compared to the Zn host atoms. The number of atoms in the O shell is 3.3 ± 1.4. Since the number of O atoms in the first shell in bulk ZnO is four and in bulk In_2O_3 is six, the measured value suggests that the In atoms are incorporated on Zn sites in the ZnO lattice. The deficiency of atoms in the Zn_{2nd} shell as observed by EXAFS at the In K edge (see Figure 2(c)) might have the same microscopic origin as the occurrence of the defect complexes observed by PAC (see Figure 1(c)).

5. Conclusion

Up to a relative In concentration of 10^{-4}, PAC investigations performed at heavily In doped nano-ZnO show that about 12% of the ^{111}In atoms are incorporated on substitutional Zn sites. At the relative In concentration of 10^{-4}, however, new In defect complexes are visible in the PAC spectra, which finally at a relative In concentration of 10^{-3}dominate the spectra. It is concluded that the In defect complexes are formed if there are more than one In atom per ZnO nanocrystal.

EXAFS measurements performed at the K edge of the Zn atoms show that the crystal structure of nano-ZnO is very close to the structure of bulk ZnO. EXAFS measurements performed at the K edge of In in heavily In doped nano-ZnO exhibit an expansion of the crystal lattice to the first O shell. Since nearly four O atoms are detected in the first shell it is suggested that the In atoms are incorporated substitutionally in the ZnO host The second Zn shell and higher are almost invisible, which might have the same microscopic origin as the defect complexes observed in the PAC experiments. Further experiments are necessary in order to establish this correlation on an atomic scale.

Acknowledgements

The financial support by the DFG within the SFB 277 is gratefully acknowledged. The authors are grateful to the HASYLAB staff for their assistance in the EXAFS experiments.

References

1. Alivisato A. P., *Science* **271** (1996), 933.
2. Shim M., Wang C., Norris D. J. and Guyot-Sionnest P., *MRS Bull.* **26** (2001), 1005.

3. Rockenberger J., zum Felde U., Tischer M., Tröger L. Haase M. and Weller H., *J. Chem. Phys.* **112** (2000), 4296.
4. Fujii M., Mimura A., Hayashi S., Yamamoto Y. and Murakami K., *Phys. Rev. Lett.* **89** (2002), 206805.
5. Agne T., Guan Z., Hempelmann R., Li X. M., Natter H., Wolf H. and Wichert T., *Appl. Phys. Lett.* **83** (2003), 1204.
6. Wichert T. In: Stavola M. (ed.), *Identification of Defects in Semiconductors*, Academic, London, 1999, p. 297.
7. Agne T., Guan Z., Li X. M., Wolf H. and Wichert T., *Phys. Status Solidi B* **229** (2002), 819.
8. Dierstein A., Natter H., Meyer F., Stephan H.-O., Kropf C. and Hempelmann R., *Scr. Mater.* **44** (2001), 2209.
9. Wolf H., Deubler S., Forkel D., Foettinger H., Iwatschenko-Borho M., Meyer F., Renn M., Witthuhn W. and Helbig R., *Mater. Sci. Forum* **10**–**12** (1986), 863.
10. Rockenberger J., Tröger L., Kornowski A., Vossmeyer T., Eychmüller A., Feldhaus J. and Weller H., *J. Phys. Chem. B* **101** (1997), 2691.
11. Ostheimer V., Ph.D thesis, Universität des Saarlandes, Saarbrücken, Germany.
12. Lany S., Ostheimer V., Wolf H. and Wichert T., *Physica B* **308**–**310** (2003), 958.
13. Rehr J. J. and Albers R. C., *Rev. Mod. Phys.* **72** (2000), 621.
14. Stern E. A., Newville M., Ravel B., Yacoby Y. and Haskel D., *Physica B* **208**–**209** (1995), 154.
15. Newville M., *J. Synchrotron Radiat.* 8 (2001), 322.
16. Rehr J. J., Albers R. C. and Zabinsky S. I., *Phys. Rev. Lett.* **69** (1992), 3397.
17. Landolt/Börnstein. In: Rössler U. (ed), *Numerical Data and Functional Relationships in Science and Technology – New Series III*. Vol. 41B, Berlin Heidelberg, New York, Springer 1999.